 doi:10.20944/preprints202101.0054.v1

Article

Physicochemical interactions in systems C.I. Direct Yellow 50 – weakly basic resins: kinetic, equilibrium, and auxiliaries addition aspects

Monika Wawrzkiewicz[1*], Ewelina Polska-Adach[1]

[1] Maria Curie-Sklodowska University in Lublin, Faculty of Chemistry, Institute of Chemical Sciences, Department of Inorganic Chemistry, M. Curie-Sklodowska Sq. 2, 20-031 Lublin, Poland; m.wawrzkiewicz@poczta.umcs.lublin.pl, ewelina.polskaadach@poczta.umcs.lublin.pl
Correspondence: m.wawrzkiewicz@poczta.umcs.lublin.pl

Abstract: Intensive development of many industries, including textile, paper or plastic, which consume large amounts of water and generate huge amounts of wastewaters containing toxic dyes, contribute to pollution of the aquatic environment. Among many known methods of wastewater treatment, adsorption techniques are considered as the most effective. In the present study the weakly basic anion exchangers such as Amberlyst A21, Amberlyst A23 and Amberlyst A24 of the polystyrene, phenol-formaldehyde and polyacrylic matrices were used for C.I. Direct Yellow 50 removal from aqueous solutions. The equilibrium adsorption data were well fitted to the Langmuir adsorption isotherm. Kinetic studies were described by the pseudo-second order model. The pseudo-second order rate constants were in the range of 0.0609-0.0128 g/mg·min for Amberlyst A24, 0.0038-0.0015 g/mg·min for Amberlyst A21 and 1.1945-0.0032 g/mg·min for Amberlyst A23, and decreased with the increasing initial concentration of dye from 100-500 mg/L, respectively. There were observed auxiliaries (Na_2CO_3, Na_2SO_4, anionic and non-ionic surfactants) impact on the dye uptake. The polyacrylic resin Amberlyst A24 can be promising sorbent for C.I. Direct Yellow 50 removal as it is able to uptake 666.5 mg/g of the dye compared to the phenol-formaldehyde Amberlyst A23 of the 284.3 mg/g capacity.

Keywords: Amberlyst, anion exchanger, direct dye, removal, resins, sorption, wastewaters

1. Introduction

Water is indispensable for life. Every organism contains water and needs it to live. The land is covered with 71% of water, where the vast majority about 97% is in the seas and oceans and is inaccessible to human consumption, while the remaining 3% is occupied by fresh water (ice sheets, glaciers, eternal snow and ground ice as well as underground water). Of these 3%, only 0.06% is easily accessible to plants, animals and humans.

The rapid increase in the world numbers and extensive industrial activities have caused that the demand for water doubles globally every 21 years. Nearly over 80 countries, representing 40% of the world's population, are struggling with water crises. The United Nations estimated that by 2025 water shortages could affect as many as 2.7 billion people. What is more, many of these countries suffer from with a lack of pure water. About 5-10 million people die annually from diseases associated with the consumption of polluted water. The demand for water grows every year, therefore it is necessary to search for more and more modern, and also economical technologies for water/wastewater treatment. Reclamation, recycling and reuse of wastewater are necessary to meet the requirements for irrigation water, industry and domestic applications due to the growing population [1-3]. Sewages are constituted by water used for specific purposes and contain various types of industrial, agricultural and urban pollution that must be removed before water re-entering into the environment. Untreated sewages cause contamination

 doi:10.20944/preprints202101.0054.v1

of surface and underground water and excludes it from economic and social uses. The most hazardous environmental pollutants are included in industrial sewages and contain mostly organic and inorganic compounds, such as dyes, phenolic and aromatic compounds as well as heavy metals [4, 5]. In the textile effluents, auxiliary agents such as salts, acids, alkalis, surfactants and oxidants can also be present [6-9]. So removing dyes and other chemicals from wastewaters is of great importance in the field of water purification. The basic treatment methods of textile wastewaters can be divided into four groups: mechanical, biological, chemical and/or physical methods (e.g. oxidation, flocculation, flotation, adsorption [10-15]) and combination of the previously mentioned ones. One of the most effective method with a great potential for removal of dyes from wastewaters are adsorption techniques [16-18]. The effectiveness of the adsorption process depends mainly on the selection of the appropriate adsorbent and the conditions under which the process is run. The most commonly used sorbent is activated carbon due to the large specific surface area, developed porous structure, possibility of modification and reactivity [19-24]. Its disadvantage is the relatively high price, which limits its use to some extent. One of the sorbents used in the purification processes are those produced from waste materials (low-cost adsorbents) [25]. Some of these materials are formed from waste substances that no longer have any use, e.g. peels, citrus stones, agricultural waste, fly ash, peat, slag and many others [26-30]. They are mainly characterized by their availability and cheap production cost, while their disadvantage is the relatively low sorption capacity. Among the various types of sorbents there are also ion exchange resins, which due to properties such as large sorption capacity, good chemical resistance, high mechanical strength, high efficiency and no loss of sorbent in the regeneration process are now of a major interest. In addition, owing to the introduction of macroporous ion exchangers with a sponge-like structure into the industry, it was possible to improve the kinetic sorption parameters of these resins [31]. The use of a given ion exchanger depends on the type of its functional groups which are responsible for ion exchange and determine the optimum efficiency of a given resin at various solution pH. In a large group of ion exchangers, anion exchangers with different basicity of functional groups found the largest practical application in the sorption process of acid, direct and reactive dyes [32-36]. An important parameter affecting the efficiency of dyes retention is also matrix composition (polyacrylic, polystyrene, phenol formaldehyde) and porosity.

The purpose of the paper was to assess the efficiency of C.I. Direct Yellow 50 uptake from aqueous solutions by the weakly basic anion exchangers differing in matrix composition. Kinetic and equilibrium parameters of the sorption process were determined and the influence of such factors as time, concentration or pH on the efficiency of dye adsorption from solutions containing additional salts and surfactants was evaluated. Anion exchange resins regeneration was evaluated, too.

2. Materials and Methods

2.1. Adsorbents and adsorbate

There were used three weakly basic anion exchange resins of different matrices: polystyrene Amberlyst A21 (abbr. A21), polyacrylic Amberlyst A24 (abbr. A24) and phenol-formaldehyde Amberlyst A23 (abbr. A23) (Figure 1). The resins were purchased from Sigma-Aldrich (Germany). Prior to the adsorption test, the resins were washed with 1 M HCl and distilled water to remove impurities and to change the ionic form to the chloride one. Resins were dried at room temperature to constant weight. The stock solution of the textile dye C.I. Direct Yellow 50 (abbr. DY50) (Boruta-Zachem, Poland) was prepared using distilled water (Figure 1). Direct dyes are salts of sulfonic acids that are characterized by good solubility in water. When dissolved in water, they dissociate into colorful anions. Direct dyes have a strong affinity for cellulose fibers due to van der Waals and hydrogen interactions. The large color scale, low price and light resistance have contributed to their use in the textile industry.

Preprints (www.preprints.org) | NOT PEER-REVIEWED | Posted: 4 January 2021 doi:10.20944/preprints202101.0054.v1

2.2. Other chemicals

Sodium sulphate and carbonate, hydrochloric acid, and sodium hydroxide were purchased from Avanor Performance Materials (Poland). The anionic surfactant sodium dodecyl sulfate (SDS) and nonionic surfactant Triton X-100 (TX-100) were purchased from Sigma-Aldrich (Germany).

2.3. Batch adsorption method

In the batch method, conical flasks closed with a silicone stopper were used. 50 mL of dye solution of appropriate concentration and 0.5 g of the anion exchanger were added. The flasks were placed in Elphin+ 358S mechanical shaker (Elphin, Poland) with a vibration amplitude of 8 units and rotary of 180 cycles/min at 25 °C and mixed from 1 to 240 min (kinetic studies) or 24 h (equilibrium studies). After shaking, the resin was separated from the solution and concentration of DY50 was measured spectrophotometrically (UV-Vis spectrophotometer Cary 60, Agilent, USA) at the maximum absorbance wavelength. The effects of Na_2CO_3 and Na_2SO_4 as well as SDS and TX-100 additions on DY50 sorption process on Amberlyst A21, Amberlyst A23 and Amberlyst A24 were studied using the following conditions (Table 1).

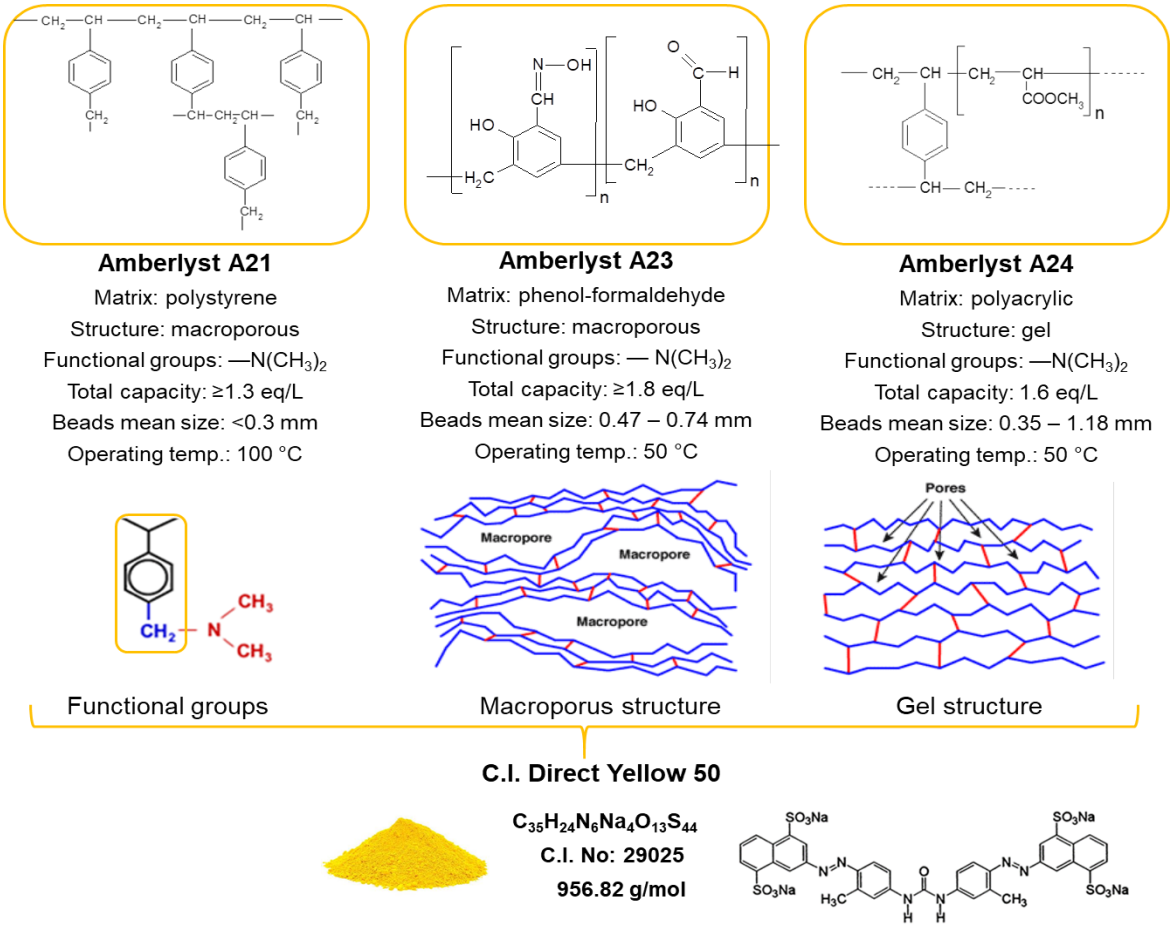

Figure 1. Physicochemical properties of the anion exchangers and dye.

Preprints (www.preprints.org) | NOT PEER-REVIEWED | Posted: 4 January 2021 doi:10.20944/preprints202101.0054.v1

Table 1. Adsorption process conditions in the systems containing salts and surfactants.

Conditions	System	
	Na_2SO_4/Na_2CO_3	SDS/TX-100
Salts/surfactants concentration (g/L)	5, 15, 25	0.1, 0.25, 0.5
Dye concentration (mg/L)	500	500
Time (min)	15	15
Volume (mL)	50	50
Anion exchanger mass (g)	0.5	0.5
Temp. (°C)	25	25
Vibration amplitude, rotary (cycle/min)	8, 180	8, 180

The effect of initial pH of the solution on the adsorption effectiveness of DY50 on the weakly basic resins A21, A23 and A24 was investigated by shaking 0.5 g of the resin with 50 mL of a solution of different initial pH containing 500 mg/L of dye. The pH was adjusted with 1 M NaOH and 1 M HCl. After the sorption process (t = 15 min), the DY50 concentration was measured spectrophotometrically.
The batch adsorption/desorption experiments were done three times, the average values are given in the figures and tables. Maximum error was found to be ±3%.

2.4. Kinetic experiments

The amount of dye adsorbed at time t (q_t) (t = 1-240 min.) was calculated from the Equation (1):

$$q_t = \frac{(C_0 - C_t)}{m} V \quad (1)$$

where: C_0 – initial DY50 concentration (mg/L), C_t – DY50 concentration after sorption time t (mg/L), V – volume (L), m – anion exchanger mass (g).

For the description of experimental data three popular models were applied based on which the kinetic parameters were calculated.

2.4.1 Pseudo first-order model (PFO)

The Langergren (1898 [37]) model of the first order is determined by the following formula (2):

$$log\ (q_e - q_t) = log\ q_e - \frac{k_1}{2.303} \quad (2)$$

where: k_1 – pseudo-first order rate constant (1/min), t – time (min), q_e, q_t – amounts of DY50 adsorbed at equilibrium and after time t (mg/g).

From the slopes and intercepts of the plots $\log(q_e - q_t)$ vs t, k_1 and q_e were calculated.

2.4.2 Pseudo second-order model (PSO)

This model proposed by Ho and McKay [38] in 1998 is represented by the following expression (3):

$$\frac{t}{q_t} = \frac{1}{k_2 q_e^2} + \frac{1}{q_e} t \quad (3)$$

Preprints (www.preprints.org) | NOT PEER-REVIEWED | Posted: 4 January 2021 doi:10.20944/preprints202101.0054.v1

where: k_2 – pseudo-second order rate constant (g/mg·min), t – time (min), q_e, q_t – amounts of DY50 adsorbed at equilibrium and after time t (mg/g).

If the kinetics of the sorption process is described by the PSO model, the t/q_t vs t graph is linear and q_e and k_2 can be determined from the slop and intercept.

2.4.3 Weber and Morris intraparticle diffusion model (ID)

Due to the porosity of the anion exchange resins the intraparticle diffusion model proposed by Weber and Morris [39] was considered in order to describe if the diffusion mechanism can be controlling step of the reaction. The Equation (4) assumes the proportionality of sorption to the square root from the time of adsorbent-solution phase contact:

$$\boldsymbol{q_t = k_i t^{0.5} + c} \quad (4)$$

where: q_t – amount of DY50 adsorbed at time t (mg/g), k_i – intraparticle diffusion rate constant (mg/g·min$^{0.5}$), c – constant illustrating the effect of the boundary layer on the sorption process, t – time (min).

2.5. Equilibrium experiments

The amount of dye adsorbed at equilibrium (q_e) was calculated from Equation (5) :

$$\boldsymbol{q_e = \frac{(C_0 - C_e)}{m} V} \quad (5)$$

where: C_0 – initial DY50 concentration (mg/L), C_e – DY50 concentration at equilibrium (mg/L), V – volume (L), m – anion exchanger mass (g).

Adsorption isotherms are used to determine the balance between the concentration of adsorbate in the solid phase and its concentration in the liquid phase. Based on the course of the isotherm, information about the maximum adsorption capacity of the sorbent can be obtained. The most commonly used models are Langmuir and Freundlich ones.

2.5.1 Langmuir model

The Langmuir isotherm equation describes chemical adsorption. The adsorbed substance forms a monomolecular film on the surface of the solid phase. The Langmuir adsorption isotherm is the basic and most widespread adsorption equation that can be considered as the initial equation for a number of more detailed studies [40, 41]. The linear form of the Langmuir isotherm is given below (6):

$$\boldsymbol{\frac{C_e}{q_e} = \frac{1}{Q_0 b} + \frac{C_e}{Q_0}} \quad (6)$$

where: C_e – equilibrium DY50 concentration (mg/L), Q_0 – monolayer capacity (mg/g), b – Langmuir constant (L/mg), q_e – amount of DY50 adsorbed at equilibrium (mg/g).

A characteristic feature of the Langmuir isotherm is the dimensionless separation factor R_L which can be calculated as follows (7):

$$\boldsymbol{R_L = \frac{1}{1 + bC_0}} \quad (7)$$

where: C_0 – initial DY50 concentration (mg/L), b – Langmuir constant (L/mg).

Preprints (www.preprints.org) | NOT PEER-REVIEWED | Posted: 4 January 2021 doi:10.20944/preprints202101.0054.v1

In addition, the value of the dimensionless R_L coefficient determines the shape of the isotherm: unfavourable ($R_L > 1$), linear ($R_L = 1$), favourable ($0 < R_L < 1$) or irreversible ($R_L = 0$) [42].

2.5.2 Freundlich model

The Freundlich (1906) isotherm equation describes the well adsorption on heterogeneous surfaces (non-uniform energy) and microporous adsorbents. It is used for description of reversible adsorption and is not confined to the formation of a single layer. The Freundlich model can be described based on the following Equation (8):

$$\boldsymbol{log\ q_e = log\ k_F + \frac{1}{n} log\ C_e} \quad (8)$$

where: k_F – Freundlich constant ($mg^{1-1/n}\,L^{1/n}/g$), $1/n$ – parameter characterizing the energy heterogeneity of the adsorbent surface, C_e – equilibrium DY50 concentration (mg/L), q_e – amount of DY50 adsorbed at equilibrium (mg/g).

The value $1/n > 1$ indicates a weak bond between the adsorbate and adsorbent molecules while a value of $1/n < 1$ points out to a strong adsorption bond as a result of strong intermolecular attractions in the adsorbent layers [43].

2.5.3. The attenuated total reflectance Fourier transform infrared spectroscopy

To investigate the dye adsorption mechanism by the anion exchanger, the attenuated total reflectance Fourier transform infrared spectroscopy (ATR-FT-IR) technique was used (Cary 630, Agilent, USA). The spectra of anion exchangers before and after DY50 sorption were recorded in the range of 600 - 3500 cm^{-1}.

2.6. Desorption experiments

Samples of resins A21, A23 and A24 (0.5 g) loaded with DY50 (50 mg/g) were shaken with 50 mL of various regenerant solutions: 1 M NaOH, 1 M HCl, 1 M NaCl, as well as theirs mixture with 50% v/v methanol. The suspensions were stirred for 3 h at a constant speed (180 cycle/min) and amplitude (A = 8). The concentration of desorbed dye was determined by absorbance analysis. The dye desorption rate (% D) was calculated from the Equation:

$$D = \frac{m_{des}}{m_{ads}} \times 100\% \quad (9)$$

where: m_{des} – mass of DY50 desorbed (mg), m_{ads} – mass of DY50 adsorbed (mg).

3. Results and Discussion

3.1. Effects of initial dye concentration and phase contact time

Kinetic sorption studies of DY50 on the Amberlyst A21, Amberlyst A23 and Amberlyst A24 anion exchangers of different matrices were estimated varying phase contact times (1-240 min) for three different initial dye concentrations (100 mg/L, 300 mg/L, 500 mg/L) at room temperature with a constant mass of anion exchanger 0.5 g and a volume of dye solution (50 mL). An increase in the initial dye concentration from 100 to 500 mg/L causes an increase in the amount of dye adsorbed by the anion exchanger (q_t) as presented in Figure 2.

Preprints (www.preprints.org) | NOT PEER-REVIEWED | Posted: 4 January 2021 doi:10.20944/preprints202101.0054.v1

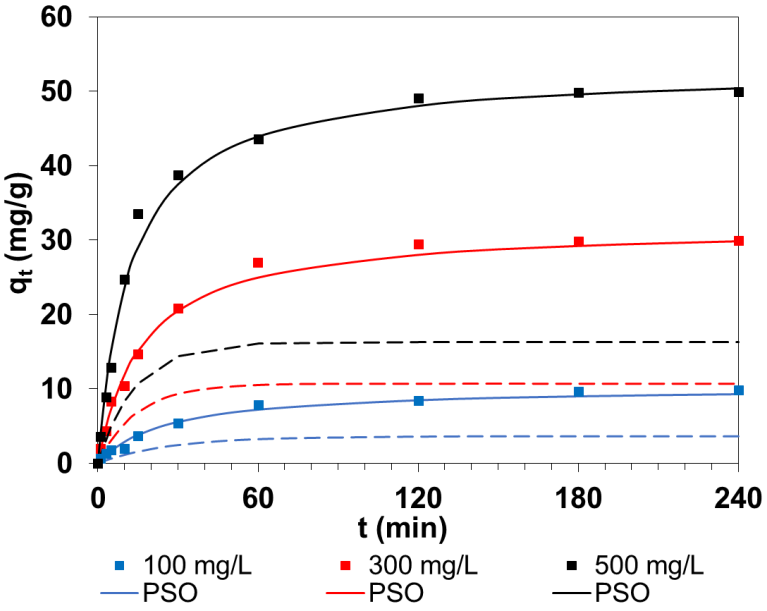

(a)

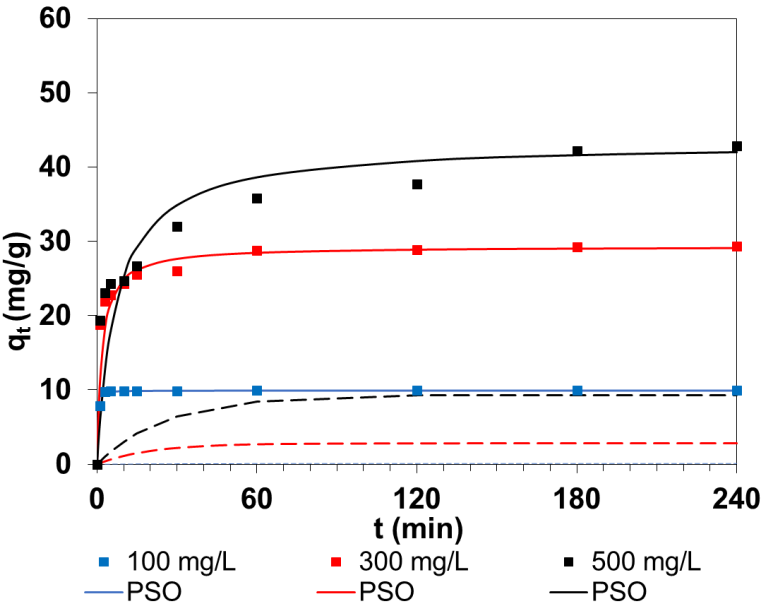

(b)

Preprints (www.preprints.org) | NOT PEER-REVIEWED | Posted: 4 January 2021 doi:10.20944/preprints202101.0054.v1

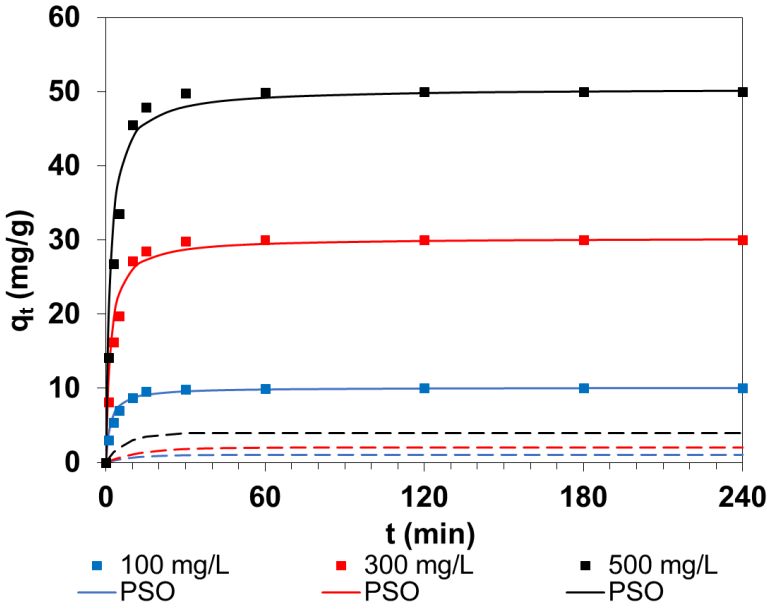

(c)

Figure 2. Influence of phase contact time and initial concentrations of DY50 on the amount of dye adsorbed by **(a)** A21, **(b)** A23 and **(c)** A24 resins and the fitting of experimental data to the kinetic models.

In the case of dye solution of 100 mg/L concentration, the time needed for its removal is quite short being: 10 min, 30 min, and 180 min for A23, A24 and A21, respectively. At the initial stage, adsorption is rapid, which indicates the presence of many readily accessible ion exchange sites on the surface of the anion exchanger. When the adsorption of the outer surface reaches saturation, the DY50 anions enter the pores of the anion exchanger and are adsorbed in the inner surface of the particle. After this time, the equilibrium is reached without a significant change of q_t values. With an increase in the amount of dye in the aqueous phase, the time needed to reach equilibrium increases, at the dye concentration of 500 mg/L it is equal to 70 min, 190 min and 220 min for A24, A23 and A21, respectively. DY50 sorption on A23 was slow compared to that on A21 and A24. For the initial concentrations of DY50 at the level of 100, 300 and 500 mg/L, q_t being 9.9 mg/g, 29.3 mg/g and 43.2 mg/g, respectively. A similar phenomenon was observed by Wawrzkiewicz [44] in the process of C.I. Direct Red 75 sorption on the weakly basic (Amberlite IRA67) and strongly basic (Amberlite IRA458) anion exchangers of polyacrylic matrix from an aqueous solution. The time needed to reach equilibrium lengthened with the increasing concentration of dye in the water phase and for the initial concentrations of 100 mg/L, 500 mg/L and 1000 mg/L it was 30 min, 60 min and 120 min using Amberlite IRA67 and 40 min, 60 min and 120 min using Amberlite IRA458.

3.2. Kinetic parameters of sorption

Knowledge of adsorption kinetics allows directing the entire adsorption process so that its effectiveness is as high as possible. The mechanism of DY50 adsorption on AA21, A23 and A24 was described using the three most common models: pseudo-first order, pseudo-second order and intraparticle diffusion. These equations are based on the definition of the amount of substance adsorbed by a mass unit of adsorbent in a unit of time. Based on the calculated kinetic parameters, listed in Table 2, it is possible to determine which model is most compatible.

Preprints (www.preprints.org) | NOT PEER-REVIEWED | Posted: 4 January 2021 doi:10.20944/preprints202101.0054.v1

Table 2. The parameters determined from the pseudo-first order, pseudo-second order and intraparticle diffusion models in the DY50-A21, DY50-A23 and DY50-A24 adsorption systems.

Resin	C_0 (mg/L)	$q_{e,exp}$ (mg/g)	PFO			PSO			ID	
			q_e (mg/g)	k_1 (1/min)	R^2	q_e (mg/g)	k_2 (g/mg·min)	R^2	k_i (mg/g min$^{0.5}$)	R^2
A24	100	10.0	2.38	0.0435	0.779	10.12	0.0609	0.999	0.441	0.809
	300	30.0	4.65	0.0334	0.715	30.28	0.0201	0.999	1.106	0.946
	500	50.0	9.19	0.0608	0.907	50.44	0.0128	0.999	1.732	0.924
A21	100	9.8	8.3	0.0163	0.915	10.3	0.0038	0.999	0.923	0.874
	300	29.9	24.6	0.0297	0.991	31.9	0.0019	0.999	4.397	0.987
	500	49.9	37.5	0.0311	0.989	52.9	0.0015	0.999	5.612	0.874
A23	100	9.9	0.2	0.0137	0.257	9.9	1.1945	0.999	0.560	0.529
	300	29.3	6.5	0.0219	0.917	29.3	0.0188	0.999	0.668	0.789
	500	42.9	21.5	0.0169	0.944	43.2	0.0032	0.999	3.184	0.998

3.2.1 Pseudo first-order model

The Lagergren equation was not used to describe the DY50 sorption kinetics on anion exchange resins of different matrices such as A21, A23 and A24 due to the small values of the determination coefficients R^2 being in the range 0.779-0.907 for A24, 0.915-9.989 for A21 and 0.257-0.944 for A23. In addition, the calculated equilibrium capacities were much lower than those determined experimentally (Figure 2 and Table 2). Moreover, the graph $log\ (q_e - q_t)$ vs t was not linear.

3.2.2 Pseudo second-order model

Figure 3 shows the linearized form of the pseudo-second order kinetic dependence for DY50 sorption from a solution of different initial concentrations on A21, A23 and A24. If the kinetics of the sorption process is described by means of the pseudo-second order model, the plot t/q_t vs t gives a linear relationship from which q_e and k_2 can be calculated and it is not necessary to know any parameter beforehand. In the case of the pseudo second order model, the k_2 constant decreases as the concentration of dye in the aqueous solution increases. Based on the data presented in the Table 2 and Figures 2 and 3, it can be concluded that it was received the best fit of the experimental data. This is indicated by not only high values of the determination coefficient R^2 (0.999), but also by the values of $q_{e,exp}$, which are very similar to those calculated from the PSO equation. Applicability of PSO model for description of experimental data in the DY50 - cotton fiber and DY50 - natural clay and organoclay adsorbents systems was described in paper by Ismail et al. [46] and Khodaeer [47].

Preprints (www.preprints.org) | NOT PEER-REVIEWED | Posted: 4 January 2021 doi:10.20944/preprints202101.0054.v1

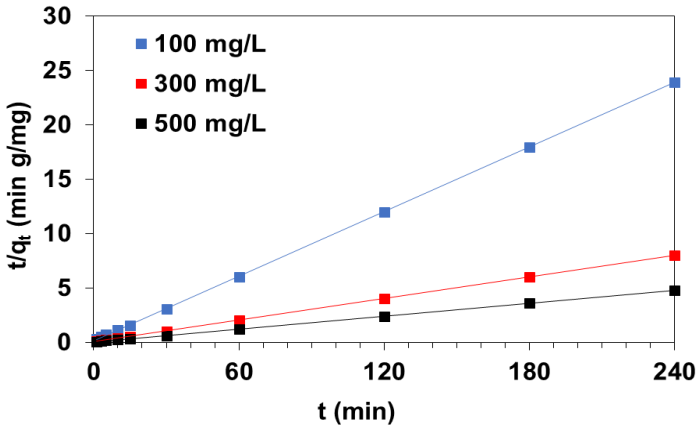

Figure 3. The t/q_t vs t dependences determined from the linear form of the PSO model in DY50 – A24 system.

3.2.3 Weber and Morris intraparticle diffusion model

Figure 4 shows the applicability of intraparticle diffusion model in description of DY50 adsorption on A21, A23 and A24. The kinetic parameters calculated from the Weber-Morris equation are given in Table 2. The graphs illustrate multi-linearity, the adsorption data can be fitted with two or three straight lines. The first part of the graph can be attributed to the diffusion effect by the boundary layer while the second linear part is associated with intraparticle diffusion (diffusion into the polymer network). The slope of the second linear part is characterized by the speed parameter corresponding to the intraparticle diffusion [45]. The values of intraparticle diffusion rate constants k_i increase in the range 0.441-1.732 g/mg·min$^{0.5}$, 0.923-5.612 g/mg·min$^{0.5}$ and 0.560-3.184 g/mg·min$^{0.5}$ with the increasing initial concentration of DY50 from 100 to 500 mg/L for A24, A21 and A23, respectively. This may be associated with a driving force that increases with the increasing dye concentration in the solution and contributes to an increase in the dye diffusion rate. The values of determination coefficients R^2 are in the range of 0.809-0.946, 0.874-0.987 and 0.529-0.998 for A24, A21 and A23, respectively.

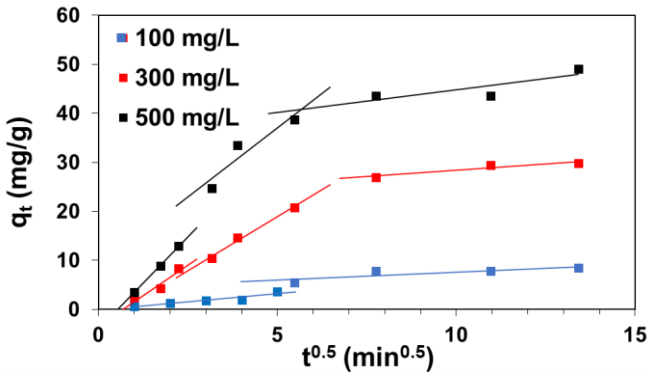

(a)

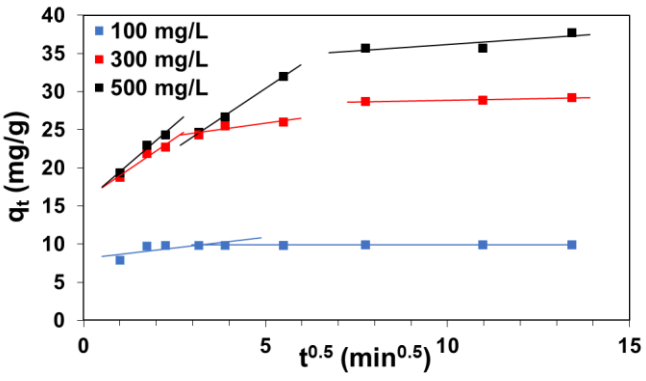

(b)

Preprints (www.preprints.org) | NOT PEER-REVIEWED | Posted: 4 January 2021 doi:10.20944/preprints202101.0054.v1

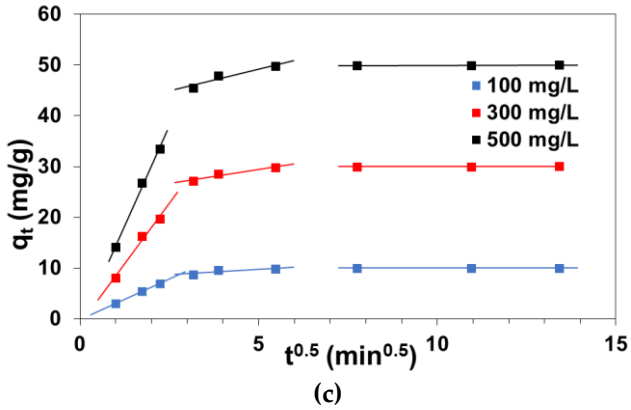

Figure 4. Intraparticle diffusion model applied for adsorption of DY50 on **(a)** A21, **(b)** A23 and **(c)** A24.

3.3. Effect of salts and surfactants presence on DY50 adsorption

Industrial wastewaters generated during various technological processes carried out in textile factories, paper and tanneries, contain auxiliary agents such as salts, acids, bases, surfactants, oxidants and reducing agents. They get in to the sewages in the amount in which they were used into the dyeing baths and do not wear out in the dyeing process of the fiber as opposed to dyes. Depending on the type and nature of the fiber, as well as the intensity of coloration, the amount of dyes and auxiliaries used are different. The compositions of dyeing baths are summarized in Table 3 [33, 34, 45].

Table 3. Compositions of baths for dyeing with direct dyes.

Bath components	Light intensity	Deep intensity
Dye	up 0.5 %	0.5-3 %
Na_2CO_3	05-1 %	1-2 %
Na_2SO_4	4-10 %	10-30 %
Surfactants	up 0.5 %	0.5-1 %

The main component of the dyeing bath is water characterized by a relatively large surface tension, therefore it is necessary to introduce surfactants which reduce surface and interfacial tension [46-47]. The addition of surfactants will cause that water will moisten the fibers surface better, which will facilitate the dyes contact with this surface. Interactions between the surfactant and the dye molecules in the aqueous solution are of great importance in the process of water treatment and reuse [48-49].
Therefore, it is necessary to assess the effects of various salt and surfactant amounts on the adsorption of dyes. The influence of auxiliaries on DY50 sorption efficiency on the A21, A23 and A24 anion exchangers was studied using the static method in the systems containing 0.5 g of anion exchangers and 50 mL of DY50 solution of 500 mg/L concentration while the concentration of salts and surfactants changed from 5 to 25 g/L of Na_2SO_4, or Na_2CO_3 and from 0.1 to 0.5 g/L of SDS or TX-100. The amount of dye adsorbed by the anion exchanger after 15 min of phase contact time was determined. In the studies a decrease of q_t was observed in the anion exchangers – DY50 systems with an increase of Na_2CO_3 concentration (Figure 5), however the least pronounced impact of carbonate presence of the uptake effectiveness can be observed for the anion exchange resin of polyacrylic matrix, i.e. A24. The decrease in the sorption capacity together with the increase of sulphate concentration in the system may be caused by competitive sorption of sulfate ions compared with the anionic form of the dye.

Preprints (www.preprints.org) | NOT PEER-REVIEWED | Posted: 4 January 2021 doi:10.20944/preprints202101.0054.v1

The presence of SDS and TX-100 (0.1-0.5 g/L) in the dye solution resulted in an increase in q_t values using the phenol-formaldehyde resin A23 during sorption test. However, the presence of these surfactants caused a decrease in the dye adsorption on the polystyrene A21 and polyacrylic A24 anion exchangers (Figure 6). The interactions between a dye and a surfactant with the same charge contribute to electrostatic interactions. The hydrophobic interactions between the DY50 and the SDS surfactant are expected to have a negative effect on dye adsorption on A21 and A24. In addition, adsorption of the SDS surfactants on the anion exchange resin may be associated with its hydrophobic nature. The alkyl chain of the surfactant can interact with aromatic rings in the acrylic-DVB or styrene-DVB matrices. The nonionic TX-100 surfactant could forms aggregates with dye molecules that were less soluble and less electronegative than the dye. On the other hand, less electronegative complexes may be less attractive for the resin anion exchanger [48].

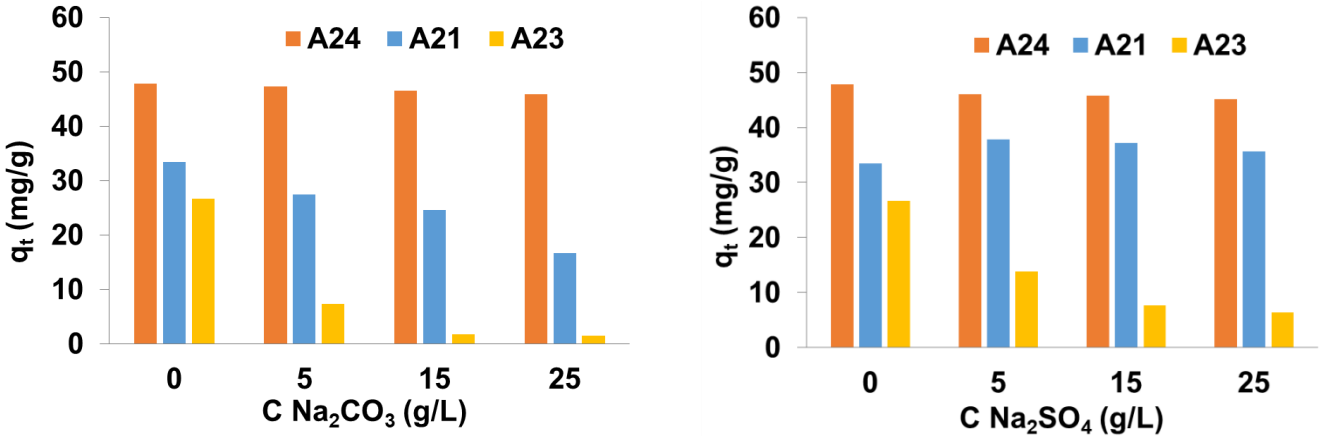

Figure 5. The effects of **(a)** Na_2CO_3 and **(b)** Na_2SO_4 presence on DY50 adsorption on A21, A23 and A24 anion exchangers.

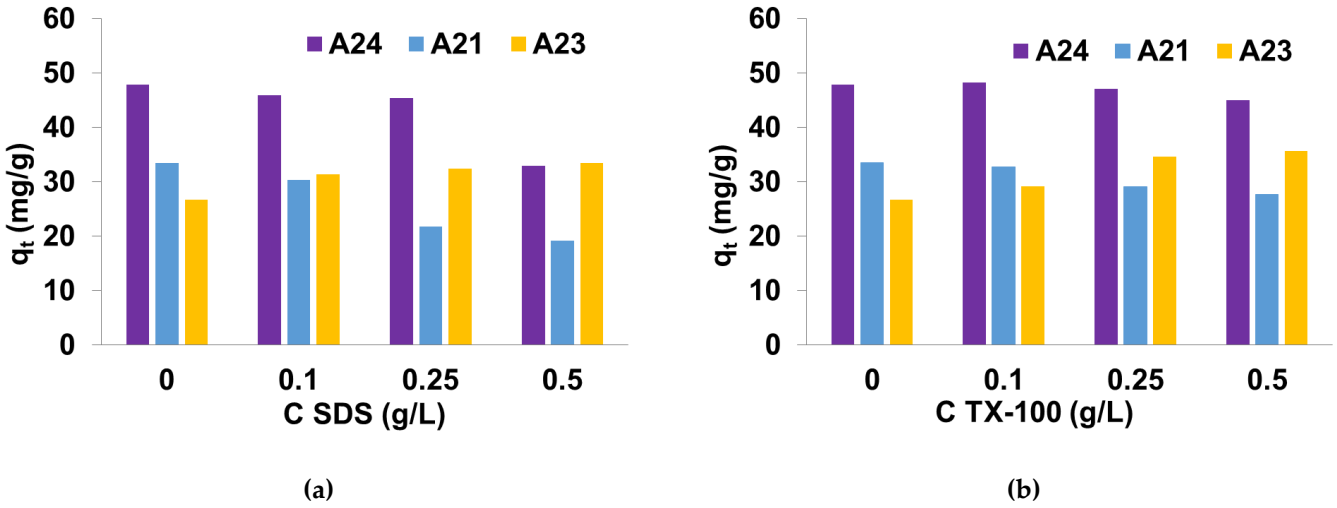

Figure 6. The effects of **(a)** anionic SDS and **(b)** non-ionic TX-100 surfactants presence on DY50 adsorption on A21, A23 and A24 anion exchangers.

3.4. Adsorption isotherms

Preprints (www.preprints.org) | NOT PEER-REVIEWED | Posted: 4 January 2021 doi:10.20944/preprints202101.0054.v1

Adsorption isotherms were determined to define the balance between the concentration of dye in the solid the liquid phases. The values of the Langmuir (Q_0 and b) and Freundlich (n and k_F) parameters obtained from the plots $log\ q_e$ vs $log\ C_e$ and C_e/q_e vs C_e along with the determination coefficients R^2 were presented in Table 4.

Table 4. The isotherm parameters determined from the Langmuir and Freundlich equations in the DY50-A21, DY50-A23 and DY50-A24 adsorption systems.

Anion exchanger	$q_{e,exp}$ (mg/g)	Langmuir			Freundlich			
		R^2	Q_0 (mg/g)	b (L/mg)	R^2	n	$1/n$	k_F ($mg^{1-1/n}L^{1/n}/g$)
A24	666.5	0.998	652.9	0.0834	0.726	6.661	0.150	239.5
A21	610.9	0.991	577.5	0.0460	0.308	3.526	0.284	84.3
A23	284.3	0.990	290.3	0.0035	0.799	1.889	0.529	4.8

3.4.1. Langmuir isotherm

It was found that the isotherms were linear over the entire range of tested concentrations, and R^2 values equaled to 0.998, 0.991, 0.990 for A24, A21 and A23, respectively. The Langmuir equation represents a better fit of experimental data than the Freundlich equation (Figure 7). The values of Langmuir parameters largely depended on the type of anion exchanger matrix. The monolayer adsorption capacity of A24 was found to be 666.5 mg/g and was larger compared A23 (Q_0=284.3 mg/g). A high b values suggest a steep isotherm onset and indicates a high affinity of the anion exchanger for the dye [11]. The b constants for A24, A21 and A23 were 0.0834, 0.0460, 0.0035, respectively. The highest value was obtained for polyacrylic Amberlyst A24 suggesting strong direct dye binding. The dimensionless separation factor R_L calculated from Equation 7 for the Langmuir type adsorption process were in the range 0 and 1 as can be seen in Figure 7.

Research conducted by Wawrzkiewicz et al. [53] concerning DY50 removal using the polyacrylic (Amberlite IRA478, Amberlite IRA958) and polystyrene (Lewatit MonoPlus MP68, Amberlite IRA900) anion exchange resins of different basicity of functionalities as well as non-functionalyzed polymeric resins of polyacrylic and polystyrene matrices (Amberlite XAD7, Lewatit VPOC1064) confirm that this process depends on the composition and the structure of anion exchanger. The highest sorption capacity towards DY50 exhibited the polyacrylic anion exchanger Amberlite IRA 958 of the quaternary ammonium functional groups and it was 534.8 mg/g. Moreover, in the case of adsorption of direct dyes on polacrylic anion exchangers, one can also notice much greater efficiency of the adsorption process using weakly basic resins compared to strongly basic ones, which was confirmed in paper [54] describing adsorption of C.I. Direct Red 75 on the weakly and strongly basic gel resins of polyacrylic skeletons such as Amberlite IRA 67 and Amberlite IRA 458.

Preprints (www.preprints.org) | NOT PEER-REVIEWED | Posted: 4 January 2021 doi:10.20944/preprints202101.0054.v1

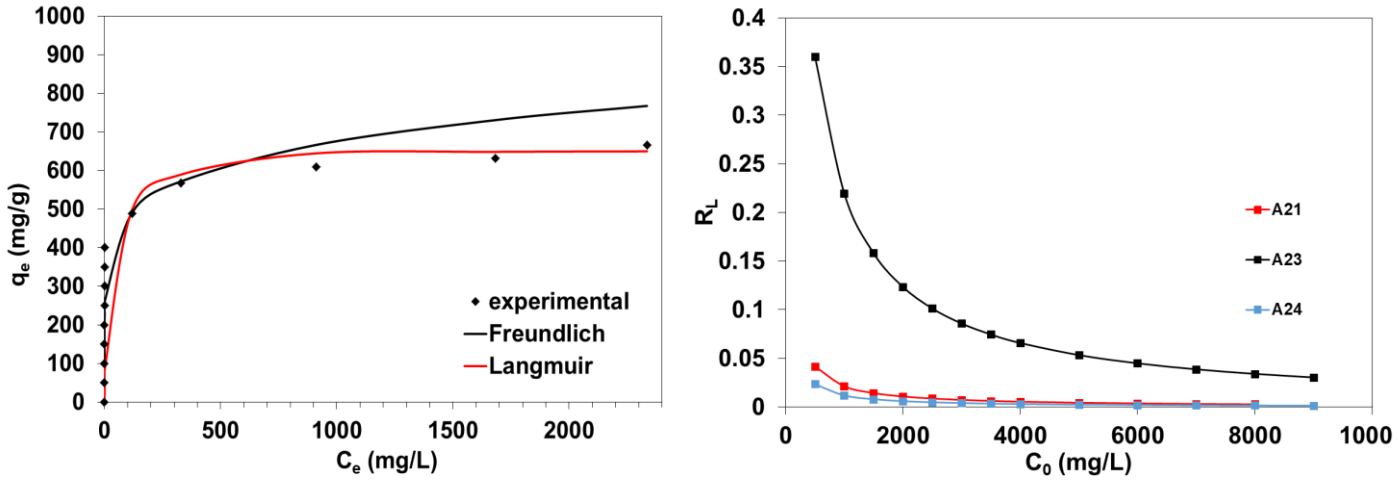

(a) **(b)**

Figure 7. Fitting of the experimental data to the Langmuir and Freundlich isotherm models in the DY50-A24 **(a)** and **(b)** the dimensionless separation factor as a function of DY50 initial concentration.

3.4.2 Freundlich isotherm

The values of determination coefficients R^2 for the Freundlich isotherm are lower than for Langmuir isotherm and are equal to 0.726, 0.308, 0.799 for A24, A21 and A23, respectively. The values *1/n* were smaller than 1, which indicates that the dye was preferably adsorbed (Table 4). In addition, k_F that is the relative sorption capacity (approximate parameter of adsorption strength) was also determined. The highest k_F value was obtained for A24 being 239.5 $mg^{1-1/n}L^{1/n}/g$. For A21 and A23, k_F were calculated as 84.3 $mg^{1-1/n}L^{1/n}/g$ and 4.8 $mg^{1-1/n}L^{1/n}/g$, respectively. The greater the value of the k_F parameter, the greater the adsorption capacity [50].

3.4. 3 Adsorption mechanism

Taking into consideration assumptions of the Langmuir and Freundlich models, calculated isotherm parameters and the structure of direct dye and anion exchange resins it can be stated that the adsorption of DY50 on A21, A23 and A24 has complex nature. The mechanism of dye retention in the anion exchanger phase occurs as a result of the formation of an ionic pair between the functional groups of the anion exchangers and the sulphonic groups of the dye in accordance with the reaction:

$$\boldsymbol{nRCH_2NH(CH_3)_2^+Cl^- + R'(SO_3^-)_n \rightarrow [RCH_2NH(CH_3)_2^+]_n(SO_3^-)_nR' + nCl^-}$$

where: $\boldsymbol{RCH_2NH(CH_3)_2^+Cl^-}$ – weakly basic anion exchanger in the chloride form, $\boldsymbol{R'(SO_3^-)_n}$ – anionic form of dye of *n* sulphonic groups

and as a result of the interaction between the delocalized electrons of benzene rings in the anion exchanger matrix and the delocalized electrons of dye aromatic rings (π-π type interactions). Not specific interactions can also be considered (Figure 8).

The mechanism of dye binding by anion exchangers depends on the chemical structure of the dye, the type and number of chromophore and auxochrome groups, as well as the structure and type of adsorbents.

Preprints (www.preprints.org) | NOT PEER-REVIEWED | Posted: 4 January 2021 doi:10.20944/preprints202101.0054.v1

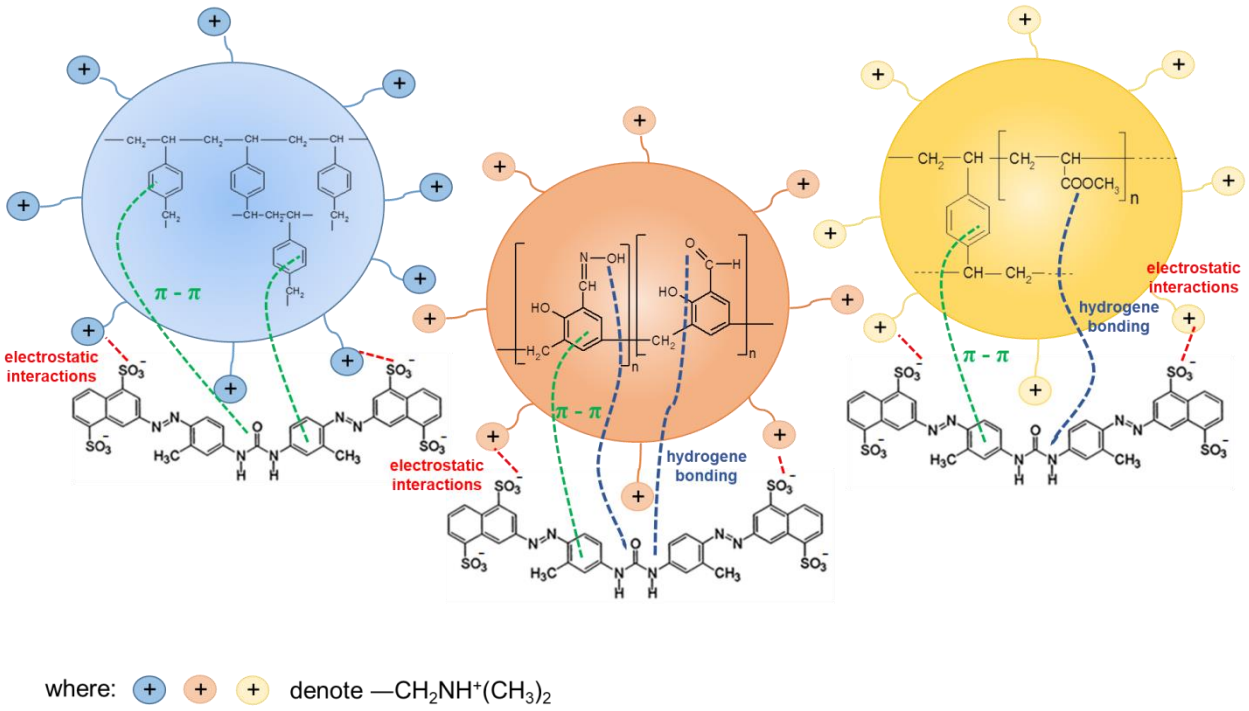

Figure 8. Proposed mechanism of DY50 interaction with the weakly basic anion exchangers of the polystyrene, phenol-formaldehyde and polyacrylic matrices.

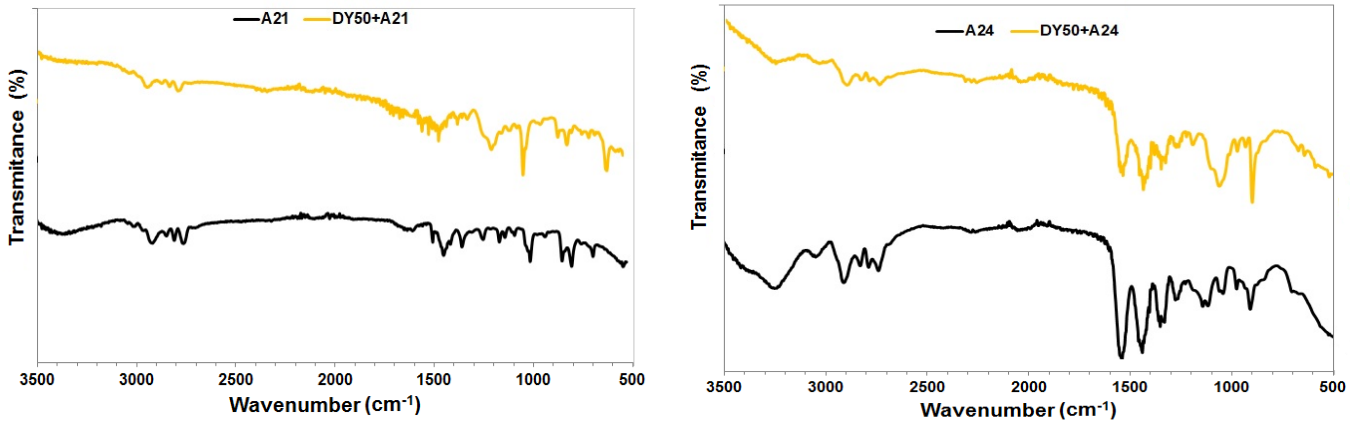

(a) **(b)**

Figure 9. ATR–FT-IR spectra of **(a)** A21 and **(b)** A24 before and after sorption of DY50.

For a more accurate analysis of DY50 retention by the A21, A23 and A24 anion exchangers there were recorded ATR-FT-IR. The spectra before and after DY50 sorption using the polystyrene (A21) and polyacrylic (A24) resins are shown in Figure 9. There were many bands characteristic for the anion exchangers matrix [55]. For example, the broad bands at 3374 cm^{-1} and 3271 cm^{-1} can be attribute to –OH stretching vibrations connected mainly with residual hydration water in A21 and A24, respectively. This band is particularly visible in the case of the polyacrylic anion exchanger, the matrix of which is more hydrophilic in comparison to the polystyrene anion exchanger, which is rather hydrophobic. There are low-intensity bands related to the stretching vibrations of the C-H in aromatic ring in the range 3100-3000 cm^{-1}. The bands at 2800-3000 cm^{-1} refer to stretching vibrations of C-H in >CH– and –CH_2–. The stretching vibrations C–C of benzene rings

Preprints (www.preprints.org) | NOT PEER-REVIEWED | Posted: 4 January 2021 doi:10.20944/preprints202101.0054.v1

and waging or twist of methylene in amine functionalities can be found at 1420-1480 cm^{-1} and 1250-1350cm^{-1}, respectively. Vibrations at 1000-1100 cm^{-1} can be attributed to C–N stretching vibrations in –NH–CH_3 as well as –CH_3 rocking in –$N(CH_3)_2$. Bands at 1085, 1145 and 1013 cm^{-1} are confirmation of a new symmetric and asymmetric vibration of the sulfonic –SO_3^- and –S=O groups in the analyzed spectra of the anion exchangers after DY50 sorption.

3.5. Impact of solution pH

The effect of the initial solution pH on the adsorption of DY50 on A21, A23 and A24 was investigated by shaking 0.5 g of the resin with 50 mL of a solution containing 500 mg/L of dye. The pH of the solution is a very important parameter controlling the sorption processes [56]. The ion exchange process depends on the acidity or alkalinity of the solution. A21, A23 and A24 are weakly basic anion exchangers for which the most effective working environment is the range of pH = 1-7. A slight decrease in sorption capacity with an increase in solution pH was noted in all cases, which can be explained by the protonation of functional groups at pH below 8-9 (Figure 10). This indicates that the mechanism of DY50 adsorption on the weakly basic anion exchangers is not only the result of interaction between resins functional groups and sulphonic groups of the dye.

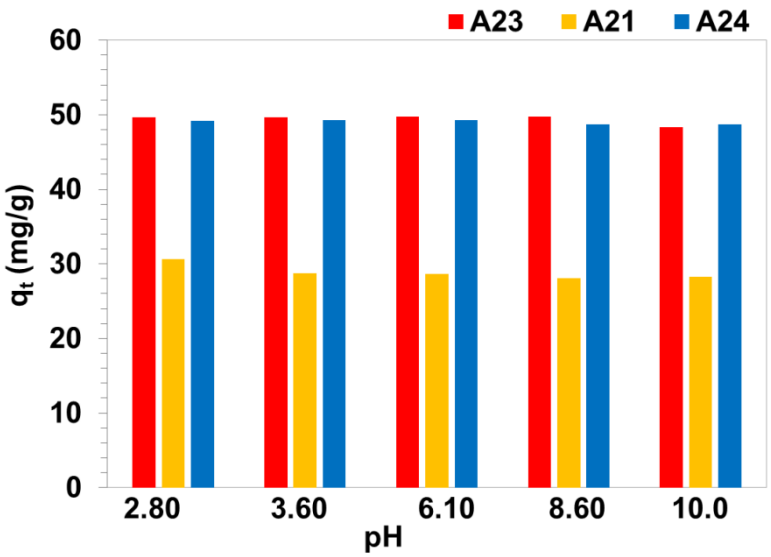

Figure 10. Influence of initial solution pH on DY50 uptake by the A21, A23 and A24 anion exchangers.

3.6. Desorption

Various reagents were tested in the experiments to find the most effective eluate: 1M NaOH, 1M HCl, 1M NaCl, 50% v/v CH_3OH, 1M NaOH + 50% v/v CH_3OH, 1M HCl + 50% v/v CH_3OH and 1M NaCl + 50% v/v CH_3OH. Figure 11 shows the results of DY50 desorption from the weakly basic anion exchangers A21, A23 and A24. The highest yield of reaction was observed during DY50 desorption from A23 and A24 using 1M NaOH + 50% v/v CH_3OH (18.76% and 18.72% for A24 and A23, respectively). It is also acceptable to use 1M NaOH for A23 (13.20%) or 1M NaCl + 50% CH_3OH for A24 (14.56%). Regenerating agents such as 1M NaCl, 1M HCl or 50% CH_3OH turn out to be ineffective (Figure 11). Comparing the values of the desorption degree in aqueous and methanol solutions, it can be concluded that the use of methanol increases the desorption efficiency. The mechanism of DY50 sorption of the weakly basic resins occurs not only through ion exchange but also as a result of strong chemical adsorption. The same conclusions were drawn in case of C.I. Direct Red 75 removal from the weakly (Amberlite IRA67) and

Preprints (www.preprints.org) | NOT PEER-REVIEWED | Posted: 4 January 2021 doi:10.20944/preprints202101.0054.v1

strongly basic (Amberlite IRA458) anion exchange resins as well as C.I. Reactive Black 5, Orange 16, Blue 15, Red 198, Red 120 from weakly (MP62) and strongly (S6328a) basic resins [45, 57].

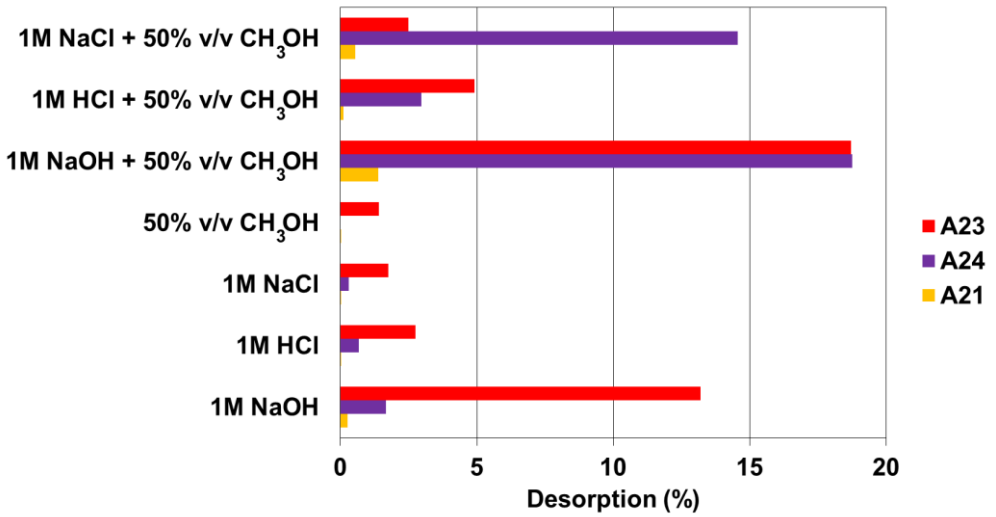

Figure 11. Desorption effectiveness of DY50 from the A21, A23 and A24 anion exchangers.

5. Conclusions

Applicability of the weakly basic anion exchangers of different matrices composition (polyarylic Amberlyst A24, polystyrene Amberlyst A21 and phenol-formaldehyde Amberlyst A23) in C.I. Direct Yellow 50 dye removal was investigated and described. Experimental parameters such as dye initial concentration, phase contact time and auxiliaries addition (Na_2SO_4, Na_2CO_3, SDS and TX-100) on dye removal efficiency are important parameters influencing the yield of dye removal. The largest sorption capacity for DY50 exhibited Amberlyst A24 (Q_0 = 666.5 mg/g) and Amberlyst A21 (Q_0 = 610.9 mg/g). Taking into account the composition of the matrix of anion exchange resins, the following series of sorbents usefulness can be presented:

polyacrylic > polystyrene > phenol-formaldehyde.

Kinetics sorption parameters were described by the pseudo-second order model and the equilibrium studies fitted well to the Langmuir equation. The resins regeneration can be performed with a yield of no more than 20% using 1 M NaOH/1 M NaCl in 50% v/v methanol. The anion exchangers can be considered as promising sorbents for removal of impurities such as dyes from aqueous solutions.

References

1. Rijsberman, FR. Water Scarcity: Fact or Fiction. *Agric. Water Manag.* **2006**, *80*, 5-22.
2. Anielak, A.M. Chemiczne i fizykochemiczne oczyszczanie ścieków. PWN Warszawa, **2002**.
3. Maciejewska-Nowak, K. Usuwanie barwników ze ścieków przemysłowych. *Ochr. Sr.* **1986**, *488/4*, 17-23.
4. Ahuja, S. Handbook of water purity and quality. IWA Publishing Great Britain **2009.**
5. Al-Asheh, S.; Banat, F.; Abu-Aitah, L. Adsorption of phenol using different types of activated bentonites. *Sep. Purif. Technol.* **2003**, *33*, 1-10.
6. Mahmoodi, N. M.; Arami, M. J. Degradation and toxicity reduction of textile wastewater using immobilized titania nanophotocatalysis. *Photochem. Photobiol. B* **2009**, *94*, 20-24.

7. Mahmoodi, N. M.; Arami, M. J. Modeling and sensitivity analysis of dyes adsorption onto natural adsorbent from colored textile wastewater. *Appl. Polym. Sci.* **2008**, *109*, 4043-4048.
8. Mahmoodi, N. M.; Arami, M. J. Bulk phase degradation of Acid Red 14 by nanophotocatalysis using immobilized titanium(IV) oxide nanoparticles. *Photochem. Photobiol. A* **2006**, *182*, 60-66.
9. Bemska, J.; Bilińska, L.; Ledakowicz, S. Analiza ścieków włókienniczych pod kątem wyboru najlepszej metody ich oczyszczania in: Z. Hubicki (ed.): Nauka i przemysł – metody spektroskopowe, nowe wyzwania i możliwości. Lublin **2012**.
10. Arica, M.Y.; Bayramŏglu, G. Biosorption of Reactive Red-120 dye from aqueous solution by native and modified fungus biomass preparations of Lentinus sajorcaju. *J. Hazard. Mater.* **2007**, *149*, 499–507.
11. Aksu, Z.; That, A.I.; Tunc¸ O. A comperative adsorption/biosorption study of Acid Blue 161: effect of temperature on equilibrium and kinetic parameters. *Chem. Eng. J.* **2008**, *142*, 23–39.
12. Cho, I.H.; Zoch, K.D. Photocatalytic degradation of azo dye (Reactive Red 120) in TiO_2/UV system: optimization and modeling using response surface methodology (RSM) based on the central composite design. *Dyes Pigments* **2007**, *75*, 533–543.
13. Tsui, S.M.; Chu, W. Photocatalytic degradation of dye pollutants in the presence of acetone. *Water Sci. Technol.* **2001**, *44*, 173–180.
14. Lee, J.W.; Choi, S.P.; Thiruvenkatachari, R.; Shim, W.G.; Moon, H. Evaluation of the performance of adsorption and coagulation process for the maximum removal of reactive dyes. *Dyes Pigments* **2006**, *69*, 196–203.
15. Golob, V.; Vinder, A.; Simoni, M. Efficiency of the coagulation/flocculation method for the treatment of dyebath effluents. *Dyes Pigments* **2005**, *67*, 93–97.
16. Shuang, Ch.; Wang, J.; Li, H.; Li, A.; Zhou, O. Effect of the chemical structure of anion exchange resin on the adsorption of humic acid: Behavior and mechanism. *J. Colloid Interface Sci.* **2015**, *437*, 163-169.
17. Mohd Salleh, M.A.; Mahmoud, D.K.; Wan Abdul Karim, W.A.; Idris, A. Cationic and anionic dye adsorption by agricultural solid wastes: a comprehensive review. *Desalination* **2011**, *280*, 1–13.
18. Bayramoglu, G.; Altintas, B.; Yakup Arica, M.; Adsorption kinetics and thermodynamic parameters of cationic dyes from aqueous solutions by using a new strong cation-exchange resin. *Chem. Eng. J.* **2009**, *152*, 339–346.
19. Valix, M.; Cheung, W.H.; McKay, G. Preparation of activated carbon using low temperaturę carbonisation and physical activation of high ash raw bagasse for acid dye adsorption. *Chemosphere* **2004**, *56*, 493–501.
20. Thinakaran, N.; Panneerselvam, P.; Baskaralingam, P.; Elango, D.; Sivanesan, S. Equilibrium and kinetic studies on the removal of acid red 114 from aqueous solutions using activated carbons prepared from seed shells. *J. Hazard. Mater.* **2008**, *158*, 142–150.
21. Akmil-Basar, C.; Onal, Y.; Kilicer, T.; Eren, D. Adsorptions of high concentration malachite green by two activated carbons having different porous structures. *J. Hazard. Mater.* **2005**, *127*, 73–80.
22. Konicki, W.; Cendrowski, K.; Chen, X.; Mijowska, E. Application of hollow mesoporous carbon nanospheres as an high effective adsorbent for the fast removal of acid dyes from aqueous solutions. *Chem. Eng. J.* **2013**, *228*, 824-833.
23. Seifikar, F.; Azizian, S.; Sillanpää, M. Microwave-assisted synthesis of carbon powder for rapid dye removal. *Mater. Chem. Phys.* **2020**, *250*, https://doi.org/10.1016/j.matchemphys.2020.123057.
24. Thamer, B.M.; Aldalbahi, A.; Moydeen, M.; El-Hamshary, H.; Al-Enizi, A.M.; El-Newehy, M.H. Effective adsorption of coomassie brilliant blue dye using poly(phenylene diamine)grafted electrospun carbon nanofibers as a novel adsorbent. *Mater. Chem. Phys.* **2019**, 234, 133-145.
25. Ahmad, A.A.; Hameed, B.H.; Aziz, N. Adsorption of direct dye on palm ash: Kinetic and equilibrium modeling. *J. Hazard. Mater.* **2007**, *141*, 70-76.
26. Bulut, Y.; Aydın, H. A kinetics and thermodynamics study of methylene blue adsorption on wheat shells. *Desalination* **2006**, *194*, 259-267.
27. Hong, G.B.; Wang, Y.K. Synthesis of low-cost adsorbent from rice bran for the removal of reactive dye based on the response surface methodology. *Appl. Surf. Sci.* **2017**, *423*, 800-809
28. Kallel, F.; Chaari, F.; Bouaziz, F.; Bettaieb, F.; Ghorbel, R.; Chaabouni, S.E. Sorption and desorption characteristics for the removal of a toxic dye, methylene blue from aqueous solution by a low cost agricultural by-product. *J. Mol. Liq.* **2016**, *219*, 279-288.
29. Zou, W.; Zhao, L.; Zhu, L. Efficient uranium(VI) biosorption on grapefruit peel: Kinetic study and thermodynamic parameters. *J. Radioanal. Nucl. Chem.* **2012**, *292*, 1303–1315.
30. Asfaram, A.; Fathi, M.R.; Khodadoust, S.; Naraki, M. Removal of Direct Red 12B by garlic peel as a cheap adsorbent: Kinetics, thermodynamic and equilibrium isotherms study of removal. *Spectrochim. Acta A.* **2014**, *127*, 415-421.
31. Dąbrowski, A.; Hubicki, Z.; Podkościelny, P.; Barczak, M. Selektywne usuwanie jonów metali ciężkich z wód oraz ścieków przemysłowych poprzez wymianę jonową. *Przem. Chem.* **2006**, *85*, 232-241.
32. Greluk, M.; Hubicki, Z. Effect of basicity of anion exchangers and number and positions of sulfonic groups of acid dyes on dyes adsorption on macroporous anion exchangers with styrenic polymer matrix. *Chem. Eng. J.* **2013**, *215–216*, 731-739.
33. Wawrzkiewicz, M.; Polska-Adach, E.; Hubicki, Z. Polacrylic and polystyrene functionalized resins for direct dye removal from textile effluents. *Sep. Sci.* **2019**, *53*, 1065-1075.
34. Wawrzkiewicz, M. Comparison of gel anion exchangers of various basicity in direct dye removal from aqueous solutions and wastewaters. *Chem. Eng. J.* **2011**, *173*, 773-781.
35. Greluk, M.; Hubicki, Z. Kinetics, isotherm and thermodynamic studies of Reactive Black 5 removal by acid acrylic resins. *Chem. Eng. J.* **2010**, *162*, 919–926.
36. Ekici, S.; Gamze Guntekin, G. Utilization of polyampholyte hydrogels for simultaneous removal of textile dyes from aqueous solutions. *Sep. Sci.* **2018**, *53*, 1777-1790.

37. http://dardel.info/IX/resin_structure.html#other
38. Lagergren, S. Zur Theorie der Sogenannten Adsorption Gelöster Stoffe, Kungliga Svenska Vetenskapsakademiens. *Handlingar* **1898**, *24*, 1-39.
39. Ho, Y.S.; McKay, G. Kinetics models for the sorption of dye from aqueous solution by wood. *Process Saf. Environ. Prot.* **1998**, *76*, 183-191.
40. Plaziński, W.; Dziuba, J.; Rudziński W. Modeling of sorption kinetics: The pseudo-second order equation and the sorbate intraparticle diffusivity. *Adsorption* **2013**, *19*, 1055-1064.
41. Hall, K.R.; Eagleton, L.C.; Acrivos, A.; Vermeulen, T. Pore and solid diffusion kinetics in fixed bed adsorption under constant pattern conditions. *IEC Fundam.* **1966**, *5*, 212-223.
42. Tan, I.A.W.; Ahmad, A.L.; Hameed, B.H. Adsorption of basic dye on high-surfacearea activated carbon prepared from coconut husk: equilibrium, kinetic and thermodynamic studies. *J. Hazard. Mater.* **2008**, *154*, 337-346.
43. Hameed, B.H.; El-Khaiary, M.I. Equilibrium, kinetics and mechanism of Malachite Green adsorption on activated carbon prepared from bamboo by K_2CO_3 activation and subsequent gasification with CO2. *J. Hazard. Mater.* **2008**, *157*, 344-351.
44. Freundlich, H.M.F. Ober dies adsorption in Losungen. *J. Phys. Chem*. **1906**, *57*, 385-470.
45. Wawrzkiewicz, M. Comparison of gel anion exchangers of various basicity in direct dye removal from aqueous solutions and wastewaters. *Chem. Eng. J.* **2011**, *173*, 773– 781.
46. Ismail, L.F.M.; Sallam, H.B.; Abo Farha, S.A.; Gamal, A.M.; Mahmoud, G.E.A. Adsorption behaviour of direct yellow 50 onto cotton fiber: Equilibrium, kinetic and thermodynamic profile. *Spectrochim. Acta A.* **2014**, *131*, 657–666.
47. Khodaeer, E.A. Removal of direct dyes from aqueous solution using natural clay and organoclay adsorbents. *Baghdad Sci. J.* **2015**, *12*, 158-166.
48. Crini, G.; Peindy, H.N.; Gimbert, F.; Robert, C. Removal of C. I. Basic Green 4 (Malachite Green) from aqueous solutions by adsorption using cyclodextrinbased adsorbent: kinetic and equilibrium studies. *Sep. Purif. Technol.* **2007,** *53*, 97–110.
49. Kowalska, I. Usuwanie anionowych substancji powierzchniowo czynnych w procesie wymiany jonowej. *Ochr. Sr.* **2009**, *31*, 25–29.
50. Majewska-Nowak, K. Usuwanie barwników organicznych z roztworów wodnych w procesie ultrafiltracji w obecności anionowej substancji powierzchniowo czynnej. *Ochr. Sr.* **2006**, *3*, 15–24.
51. Ghoreishi, S.M.; Behpour, M.; Shabani-Nooshabadi, M. Interaction of anionic azo dye and TTAB–cationic surfactant. *J. Braz. Chem. Soc.* **2009**, *20*, 460–465.
52. Khan, M.N.; Sarwar, A. Study of dye-surfactant interaction: aggregation and dissolution of yellowish in N-dodecyl pyridinum choride. *Fluid Phase Equilb.* **2006**, *239*, 166–171.
53. Wawrzkiewicz, M.; Polska-Adach, E.; Hubicki, Z. Polacrylic and polystyrene functionalized resins for direct dye removal from textile effluents. *Sep. Sci. Technol.* **2019**, *53*, 1065-1075.
54. Arami, M.; Limaee, N.Y.; Mahmoodi, N.M.; Tabrizi, N.S. Equilibrium and kinetics studies for the adsorption of direct and acid dyes from aqueous solution by soy meal hull. *J. Hazard. Mater.* **2006**, *135*, 171–179.
55. Zagorodni, A.A.; Kotova, D.L.; Selemenev, V.F. Infrared spectroscopy of ion exchange resins: chemical deterioration of the resins. *React. Funct. Polym.* **2002**, *53*, 157-171.
56. Clavijo C.; Osma, J.F. Functionalized Leather: a novel and effective hazardous solid waste adsorbent for the removal of the diazo dye congo red from aqueous solution. *Water* **2019**, *11*, 1906.
57. Karcher, S.; Kornmüller, A.; Jekel, M. Screening of commercial sorbents for the removal of reactive dyes. *Dyes Pigments* **2011**, *51*, 111-125.